Biochemistry and Biophysics Reports 30 (2022) 101231

Contents lists available at ScienceDirect

Biochemistry and Biophysics Reports

journal homepage: www.elsevier.com/locate/bbrep

R-etodolac is a more potent Wnt signaling inhibitor than enantiomer, S-etodolac

JoAnn S. Roberts [a], Chao Ma [a], Sarah Y.T. Robertson [a], Stephen Kang [a], Christiana S. Han [a], Sophie X. Deng [a,b,**], Jie J. Zheng [a,b,*]

[a] Stein Eye Institute, Department of Ophthalmology, David Geffen School of Medicine at University of California, Los Angeles, CA, 90095, USA
[b] Molecular Biology Institute, University of California, Los Angeles, CA, 90095, USA

ARTICLE INFO

Keywords:
Wnt signaling
R-etodolac
S-etodolac
Limbal stem epithelial cells

ABSTRACT

Etodolac is an FDA-approved nonsteroidal anti-inflammatory drug (NSAID) used to treat a variety of inflammatory diseases. The drug is administered as a racemate (50/50 mixture of R- and S- enantiomers), however, studies have shown that the two enantiomers have distinct biologic and pharmacokinetic differences. Wnt signaling, which plays key roles in cell proliferation, polarity, and differentiation, has been shown to be inhibited by R-etodolac; however, comparative analyses of R- and S-etodolac in this function have not been conducted. We used *in silico* molecular docking and TOPflash functional biologic assays to compare R- and S-enantiomers effect on Wnt signaling inhibition. Further, we used a cultivated limbal stem epithelial cell (cLSCs) model to investigate enantiospecific changes in the colony-forming efficiency (CFE) of cLSCs. The data shows that R-etodolac is a more potent inhibitor of Wnt signaling. In addition, consistently, while both enantiomers demonstrate a dose-dependent decrease in CFE of cLSCs, R-etodolac is a more potent inhibitor.

1. Introduction

Etodolac is a nonsteroidal anti-inflammatory drug (NSAID) widely used to treat chronic arthritis and acute pain. Similar to other NSAIDs, it potently binds and inhibits cyclo-oxygenase (Cox-1 and Cox-2), thereby preventing the formation of the prostaglandins involved in pain and inflammatory pathways. While the side effects of etodolac are typical of other NSAIDs, it can in extremely rare cases cause hepatotoxicity due to an unknown mechanism [1]. Etodolac is administered as a racemic mixture of its two enantiomers (R- and S-), but the enantiomers have distinct functions and pharmacokinetics. The inhibitory effects, mainly on Cox-2, are due to the S- enantiomer [2]. Because the two enantiomers do not readily interconvert [3], distinguishing the pharmacological targets and activities of both enantiomers is feasible and important in the improvement of etodolac for clinical use.

Etodolac, like some other NSAIDs [4], also inhibits Wnt signaling in addition to Cox-1 and -2. However, the differences between R- and S-etodolac in Wnt inhibition and their mechanism of action has yet to be investigated. The effects of racemic mixture of the enantiomers and the R- and S- enantiomers separately could have implications for stem cell maintenance, cell differentiation, cancer, and other cells and diseases affected by the Wnt pathway [5].

In the present study, we first use an *in silico* structure-based approach to evaluating the binding ability of the etodolac enantiomers to Fzd receptors. We then investigate the Wnt inhibitory effects of R- and S-etodolac and test their effect on the colony-forming ability and proliferation of cultivated human limbal epithelial stem cells (cLSCs). Because Wnt signaling is necessary for and improves the maintenance of LSCs in culture [6–8], cLSCs are an effective system to characterize the differences between R- and S-etodolac in a biological stem cell model. We demonstrate that R- and S-etodolac have different predicted kinetics of Fzd receptor binding. Our results suggest that R-etodolac is a more potent Wnt signaling inhibitor than S-etodolac. Therefore, this work has important implications in the future therapeutic use of etodolac racemate and purified chiral forms of etodolac.

* Corresponding author. Stein Eye Institute, Department of Ophthalmology, David Geffen School of Medicine at University of California, Los Angeles, CA, 90095, USA.
** Corresponding author. Stein Eye Institute, Department of Ophthalmology, David Geffen School of Medicine at University of California, Los Angeles, CA, 90095, USA.
E-mail addresses: deng@jsei.ucla.edu (S.X. Deng), jzheng@jsei.ucla.edu (J.J. Zheng).

https://doi.org/10.1016/j.bbrep.2022.101231
Received 9 November 2021; Received in revised form 28 January 2022; Accepted 7 February 2022

A

	Docking score	Glide energy
FZD8		
S-Etodolac	-4.858	-28.792
R-Etodolac	-4.011	-25.706
FZD4		
S-Etodolac	-4.042	-23.59
R-Etodolac	-4.037	-23.631
FZD7		
S-Etodolac	-3.742	-19.383
R-Etodolac	-4.128	-22.66

B

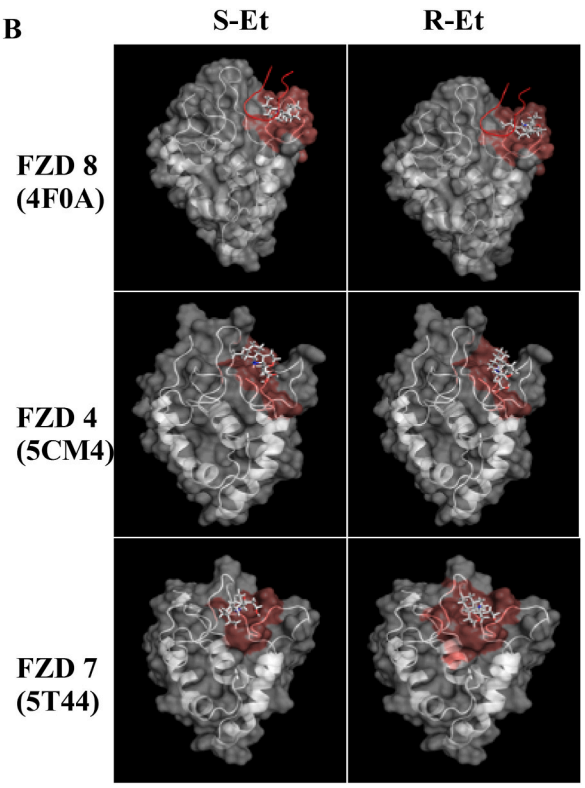

Fig. 1. In silico molecular docking of R- and S-etodolac with Frizzled receptors.
A. Docking scores and predicted glide energy of R- and S-Etodolac with Fzd 8, 4, and 7. **B**. Surface modeling of R- and S-etodolac molecules in the CRD of Fzd 8, 4, and 7 (pdb codes 4F0A, 5CM4, and 5T44, respectively). The Fzd 8 surface model depicts the Wnt ligand in the CRD binding pocket as reference for the inhibitory binding site [9].

2. Methods

2.1. Docking and scoring in virtual screening

The etodolac ligand structures were retrieved from the crystal structure of Equine Serum Albumin in complex with R- or S-etodolac (Protein Data Bank codes 5V0V, 8QS, 8QP, respectively). The etodolac enantiomers were prepared with the LIGPREP module in the Schrödinger package (Schrödinger, New York, NY). The pH was set to 7.0, and OPLS 2005 force field parameters were applied. The receptor models were derived from the mouse FZD8 CRD crystal structure (Protein Data Bank code 4F0A, chain A), the human FZD4 CRD (Protein Data Bank code 5CM4, chain A), and the human FZD7 CRD (Protein Data Bank code 5T44, chain A). Schrödinger's Protein Preparation Wizard (Schrödinger, New York, NY) was used to add missing hydrogen atoms, partial charges, fix crystal structure errors, and remove co-crystallized water molecules. The molecular mechanics force field grids were generated around the Wnt binding site using Glide. The grid for FZD8 was determined using residues that form the binding cavity [9]: Ile^{46}, Gly^{47}, Tyr^{48}, Ile^{95}, Leu^{97}, Gln^{141}, Gly^{142}, Asn^{143}, Pro^{144}, Asp^{145}, Thr^{146}, Leu^{147}, Met^{149}, Asp^{150}, and Tyr^{151}. FZD 8 (NP_114072.1). This was aligned with FZD 4 (NP_003005.2) and 7 (NP_003498.1) using Clustal Omega software to determine the residues that correspond to the binding cavity of Wnt ligand. The grid used to designate the areas for *in silico* docking was formed based on this alignment. Virtual screening was completed using the Glide module in the Schrödinger Software Release 2018-4 [10,11], at standard precision.

2.2. Cell and tissue culture

Cell Culture: 293 STF cells, a stable transfected cell line expressing luciferase under the T-cell factor/lymphoid enhancer factor (TCF/LEF) promoter was used for TOPflash experiments (ATTC CRL-3249). L-cells (ATTC CRL 2648) and L-Wnt3a (ATTC CRL 2647) were used to prepare a control conditioned media (LCM) and Wnt-conditioned media (WCM) that was used in the TOPflash assay. All cells were cultured and maintained in Dulbecco's modified Eagle's medium (DMEM) containing 10% fetal bovine serum, 100 U/mL penicillin, and 100 μg/mL streptomycin in 5% CO_2 at 37 °C. L-Wnt3a cells media was supplemented with 0.4 mg/mL G-418. *Preparation of conditioned media:* Briefly, cells were grown for 4 days without changing media in T150 flasks. L-cells and L-Wnt3a media was collected, centrifuged to remove debris, and sterile filtered (0.2 μm) before experimental use. *Human Corneoscleral Tissue:* Human LSC cultures were cultivated from two separate corneoscleral tissue donors that were obtained from different eye banks. The experimental protocol was exempted by the University of California Los Angeles Institutional Review Board (IRB#12–000363) and performed in accordance with the Declaration of Helsinki. LSCs were cultured using supplemental hormone epithelial medium (SHEM): DMEM/F12 medium supplemented with 5% fetal bovine serum (FBS; Life Technologies), N2 supplement (Life Technologies), 2 ng/mL of epidermal growth factor (EGF; Life Technologies), 8.4 ng/mL of cholera toxin (Sigma-Aldrich; St. Louis, MO), 0.5 μg/mL of hydrocortisone (Sigma-Aldrich), 0.5% final concentration of dimethyl sulfoxide (DMSO; Sigma-Aldrich), penicillin-streptomycin (Life Technologies) and gentamicin/amphotericin B (Life Technologies).

2.3. TOPflash assay

Stably transfected HEK 293 (293 STF) luciferase-based reporter cell line (ATCC, Manassas, VA), which expresses firefly luciferase under the control of TCF/LEF promoter, was used to examine the activation or inhibition effect of the small molecules (MFH-ND, MFH, and ND) on regulating the canonical Wnt signaling pathway. 293 STF cells were

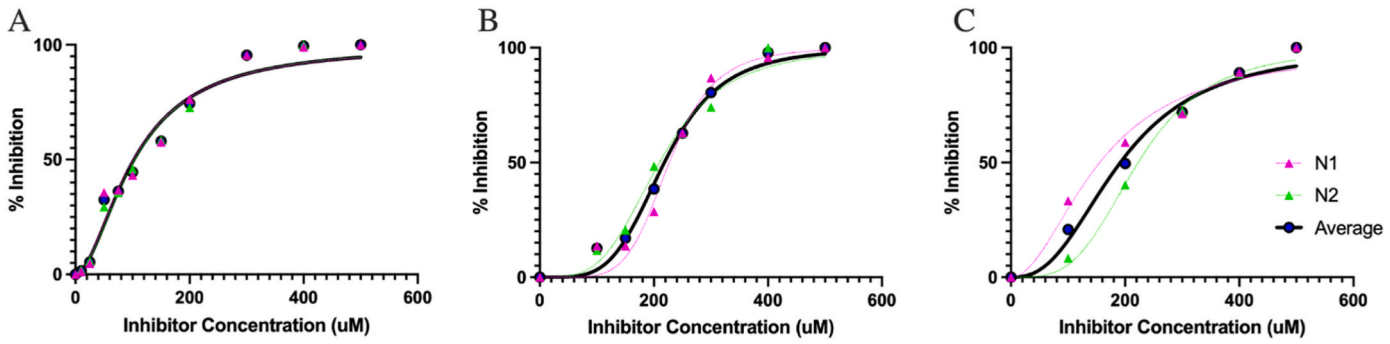

Fig. 2. Dose-dependent inhibition of Wnt signaling. TOPflash Wnt activity assays were performed after treatment (0–500 μM) with **A.** R-etodolac, **B.** S-etodolac, and **C.** Racemic etodolac. All figures show each of the two biological samples separately, N1 (magenta) and N2 (green), as well as the average of the two samples, Average (black). **A.** $IC_{50(\text{Average R-Etodolac})}$: 102.5 μM, 95% CI: 86.08 to 120.7 μM; $IC_{50(\text{N1 R-Etodolac})}$: 101.1 μM, 95% CI: 82.90 to 121.5 μM; and $IC_{50(\text{N2 R-Etodolac})}$: 103.9 μM, 95% CI: 88.84 to 120.4 μM. **B.** $IC_{50(\text{Average S-Etodolac})}$: 218.3 μM, 95% CI: 203.7 to 232.8 μM; $IC_{50(\text{N1 S-Etodolac})}$: 226.9 μM, 95% CI: 209.4 to 243.6 μM; and $IC_{50(\text{N2 S-Etodolac})}$: 209.7 μM, 95% CI: 192.2 to 227.3 μM. **C.** $IC_{50(\text{Average Racemic Etodolac})}$: 191.7 μM, 95% CI: 157.0 to 227.1 μM; $IC_{50(\text{N1 Racemic Etodolac})}$: 155.6 μM, 95% CI: 111.3 to 198.9 μM; and $IC_{50(\text{N2 Racemic Etodolac})}$: 222.9 μM, 95% CI: 204.8 to 240.5 μM. Figures and IC_{50} were determined using Graphpad Prism (version 9.3.1). (For interpretation of the references to colour in this figure legend, the reader is referred to the Web version of this article.)

cultured in 5% CO2 at 37 °C in Dulbecco's modified Eagle's medium supplemented with 4.5 g/L D-glucose and 2 mM glutamine (DMEM, Invitrogen, Carlsbad, CA) containing 10% fetal bovine serum (FBS, Invitrogen), 0.1 mM nonessential amino acids (Gibco), and 10 mM HEPES (Gibco). 293 STF cells were seeded and grown overnight in a 96-well plate at 2×10^5 cells/well confluence. In either control conditioned media or Wnt3a-conditioned media, cells were incubated with one of the following reagents: Racemic Etodolac (Sigma Aldrich), R-etodolac, or S-etodolac (Toronto Chemicals), dissolved in DMSO (from 0 to 500 μM range). After 16 h of incubation, the cells were incubated for 30 min with a cell-permeant fluorogenic substrate used to measure cell viability and normalize for potential toxic effects of the molecules. 5′-fluoroluciferin, which is cleaved by luciferase thereby emitting luminescence, was then added to the cells. Both fluorescence and luminescence were measured using a BioTek microplate reader according to manufacturer's protocol. Each experiment was performed in biological duplicates and technical triplicates (N = 6 total). The luminescence values are presented as the average of two experiments a ratio relative to the DMSO-only control. Analysis of the R and S-Etodolac dose-response data and calculation of IC_{50} values were performed using Prism.

2.4. Colony forming efficiency

Isolated single limbal epithelial cells were seeded at a density of 200 cells/cm^2 on mitomycin-treated 3T3-J2 mouse fibroblasts (3T3; the Howard Green laboratory, Harvard Medical School, Sigma-Aldrich; St. Louis, MO) for 2 h at 37 °C. LSCs were cultivated in SHEM medium and refed every 2-days with the R- or S- Etodolac treatment (25, 85, or 200 μM) dissolved in DMSO. Each well had the same final DMSO concentrations of 0.5%. cLSCs were fixed with 4% paraformaldehyde (ThermoFisher Scientific, Carlsbad, CA, USA) and stained for 15 min with 0.5% rhodamine B (Sigma-Aldrich Corp.) at room temperature. Each experiment was performed in biological and technical triplicates and the number of colonies determined using ImageJ Software. The number of colonies formed were then divided by the number of cells plated to obtain the colony forming efficiency (CFE).

2.5. Statistics

Data were analyzed using Student's *t*-test and error bars represent the mean ± the standard deviation. P values < 0.05 were considered statistically significant.

3. Results and discussion

Wnt signaling is ubiquitously involved in many cellular processes and disease mechanisms, including stem cell biology, embryonic development, and cancer. The family of Frizzled (Fzd) receptors are comprised of 10 mammalian genes that serve as main receptors for Wnt signaling [12]. Fzds oligomerize with LRP5/6 or ROR/RYK among other membrane-associated proteins to activate canonical and non-canonical Wnt signaling, respectively. Fzds are therefore a promising cell-surface target for therapeutic modulation of Wnt signaling, and many recent studies involve structure-based drug discovery of small molecules targeting Fzd receptors [6,13–17]. The cysteine-rich domain (CRD) of Fzd receptors is highly conserved and is the site of Wnt-ligand binding [18]. The docking scores and predicted binding free energies of the best-fit conformations of R- and S-etodolac with the CRD regions of Fzd 8, 4, and 7 are reported in Fig. 1. This data predicts that S-etodolac binds Fzd 8 slightly better than R-; R-etodolac binds Fzd 7 slightly better than S-; and both have equal predicted binding affinity for Fzd 4. Etodolac enantiomers show stereoselective binding to human serum albumin [19] and have enantioselective pharmacokinetics. However, it is currently unclear how these predicted Fzd receptor affinity differences of R- and S-etodolac may affect Wnt signaling inhibition; thus further investigation is needed to determine the specific binding affinities of etodolac enantiomers to different FZD receptors and elucidate the biological impact of the subtle predicted differences. This topic is worth exploring due to the current and continued use of etodolac as an NSAID in the treatment of acute pain (200–400 mg oral dosage) and osteoarthritis/rheumatoid arthritis (300–600 mg oral dosage [20]). The bioavailability of etodolac is 100% in solution and 80% as a tablet. After administration, the plasma levels can range from 14 ± 4 to 37 ± 9 μg/mL[20]; however it is important to note that R-etodolac remains in human plasma longer than S-etodolac when a racemate is administered [21]. Therefore, the exposure to R-etodolac is far greater than S-etodolac. Although most chiral NSAIDs undergo *in vivo* unidirectional inversion via processing in the liver by hepatic enzymes, etodolac does not show any inversion of its enantiomers [3]. This means that the biologic effect of R-etodolac is an important consideration when using a racemate for treatment of disease. A deeper understanding of the binding strength and partners of etodolac enantiomers will add important value when considering its use or the use of purified enantiomers in the treatment of disease.

We continued our investigation of etodolac enantiomers on Wnt signaling by comparing the dose-dependent inhibitory effects of the etodolac enantiomers using the TOPflash assay. The ability of etodolac to inhibit Wnt signaling has been demonstrated in previous studies

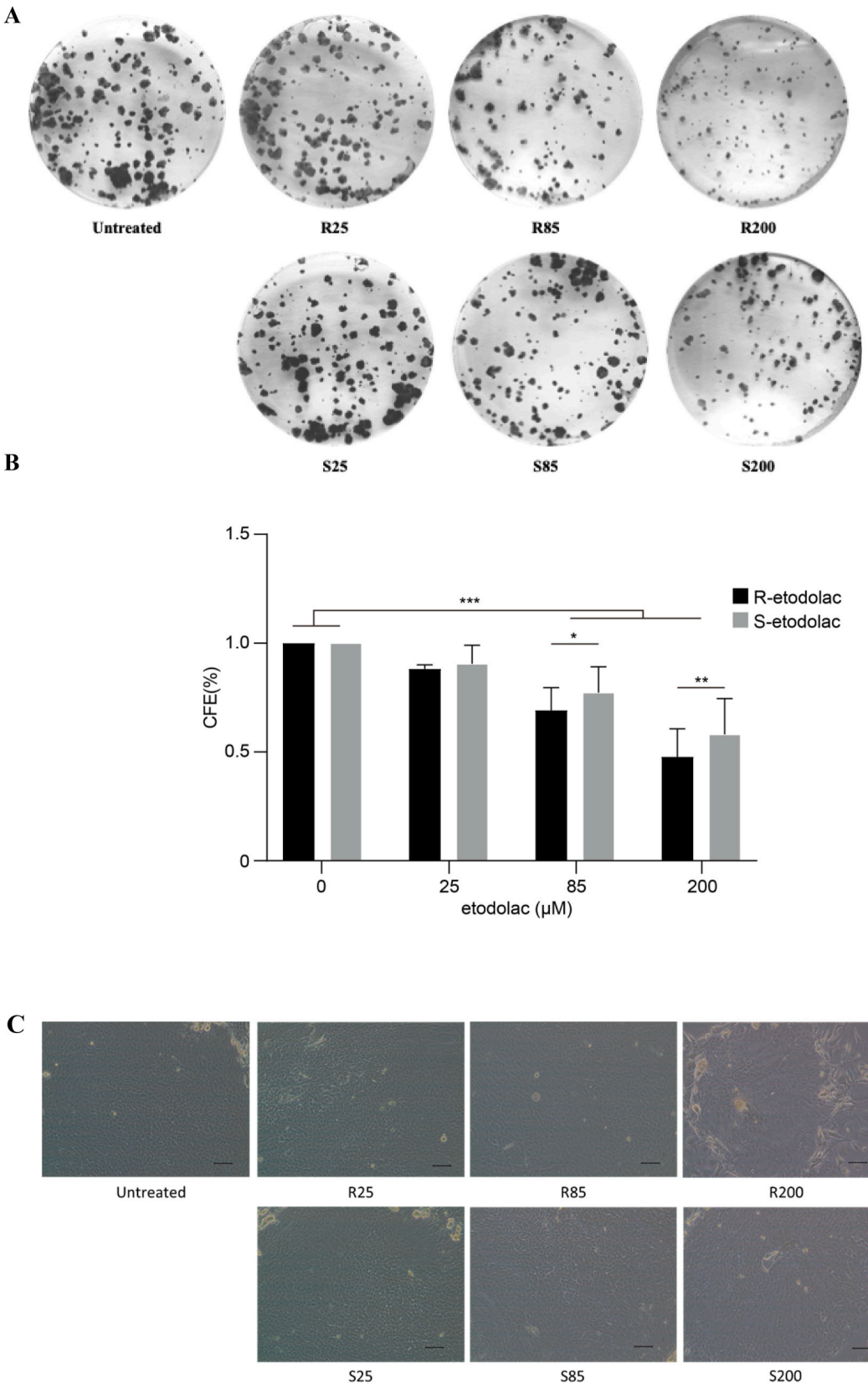

Fig. 3. Functional assay of etodolac-induced Wnt inhibition using a cultivated human limbal epithelial stem cell model. A. Representative images of rhodamine-stained cLSC colonies: untreated, R-etodolac, and S-etodolac (25, 85, or 200 μM). **B**. Quantitative analysis of colony forming efficiency of cLSCs. **C.** Micrographs of cLSC colonies treated with R- and S-etodolac (4× magnification). Mean ± SD; N = 3 biological replicates *p < 0.05, **p < 0.01, ***p < 0.001.

where it decreases active β-catenin levels and phosphorylated GSK3β levels in hepatoma and hepatoblastoma cells [22–24]. R-Etodolac also has anti-tumorigenic and cytotoxic effects in chronic lymphocytic leukemia, multiple myeloma, and prostate cancer [24–26]. However, these studies did not directly compare the inhibitory effects of R-etodolac with S-etodolac or the racemate. Furthermore, the etodolac inhibitory concentration needed to inhibit Wnt signaling by 50% (IC_{50}) is not presented in the literature. Our results reveal a marked difference between the potency of R- and S-etodolac in Wnt signaling inhibition (Fig. 2). Half maximal inhibitory concentration (IC_{50}) of S-etodolac (218.3 μM, 95%, confidence interval (CI): 203.7–232.8 μM) is ~90% higher than R-etodolac IC_{50} (102.5 μM, 95%, CI:86.08–120.7 μM). IC50 of racemate (191.7 μM, 95%, CI: 157.0–227.1 μM) is between the two. This suggests that the R-enantiomer is a more potent inhibitor of Wnt signaling.

We further extended our study to include a biologic functional assay of etodolac by assessing clonogenic ability and growth capacity of cLSCs using a colony forming efficiency (CFE) assay [27]. Wnt signaling has previously been shown to be a required regulatory pathway in maintaining an undifferentiated state of cLSCs [7,8]. Manipulation of the Wnt pathway by small molecules has led to observable differences in the CFE of cLSCs, where targeted small molecule Wnt inhibition reduced CFE and activation increased it [7,8,28]. Therefore, we used cLSCs as a system to confirm the biologic differences of R- and S-etodolac inhibition of Wnt signaling using CFE analysis of cLSCs. Comparative analysis of cLSCs treated with either R-, or S-etodolac showed that CFE is significantly diminished at 85 μM and 200 μM compare to untreated (Fig. 3). Moreover, the decrease observed in CFE is more significant in R-etodolac than S-etodolac. Visual examination of the colonies in Fig. 3A also reveals R-etodolac dose-dependent differences in colony size. The cell morphology of etodolac-treated cLSCs also shows more disorganized colonies and larger cells with higher treatments of R-compared to S-etodolac (Fig. 3C). Overall, this data further supports R-etodolac as a more potent Wnt inhibitor than S-etodolac.

Understanding enantioselective targets and mechanisms of etodolac has clear advantages. The future therapeutic use of R-etodolac as a Wnt inhibitor can minimize COX-2 dependent side effects caused by the S-enantiomer. For example, COX-2 is increased in hepatocellular carcinoma; however, COX-2 inhibition can cause cardiovascular and renal challenges. Using purified R-etodolac allows for COX-independent Wnt inhibition [26] that has anti-hepatoma effects without the side effects [23]. R-etodolac also induces cytotoxicity in myeloma cell lines [29] and has an antagonistic effect on the function of ß-catenin, which is associated with a variety of cancers. It is also important to consider that S-etodolac, which primarily inhibits COX, also inhibits Wnt to a lesser extent. The primary role of S-etodolac as an NSAID may also have a harmful side effect of inhibiting Wnt signaling in actively proliferating cell types. Early studies have used the racemate and also found anti-tumorigenic effects, however the differences between the enantiomers are not delineated [30]. Thus, this work has a broad range of therapeutic implications. As information continues to become available on the biological and pharmacokinetic differences between R- and S-etodolac, the need to separate these enantiomers in studies becomes clearer.

Wnt inhibitors that bind to the CRD region of Fzd receptors also have therapeutic implications in drug development. Molecules with structural similarities to etodolac may be used to generate Wnt mimics that bind to both the Fzd receptor and LRP 5/6 co-receptor, thereby mimicking oligomerization [6]. The understanding of etodolac chirality and its impact on the potency of Wnt inhibition may better inform the selection of molecules used in drug development.

In summary, R-etodolac significantly decreases Wnt signaling *in vitro* and is a more potent Wnt inhibitor than the S- enantiomer as demonstrated by comparative biologic analysis of their effect on cLSCs. The differences between these enantiomers should be carefully considered when the racemate is used as treatment for disease or if considering using purified chiral drugs. For example, racemic etodolac is currently being used in clinical trials as an anti-tumorigenic and anti-metastatic agent [31,32], so the enantiomeric differences should be considered in the analysis of the results from the trials. Further study of the mechanisms of action of R- and S-etodolac will delineate their specific advantages for clinical treatment of disease thereby improving therapeutic strategies for cancers, arthritis and other inflammation-related diseases.

Declaration of competing interest

The authors declare no conflict of interest.

Acknowledgements

This work was supported in part by the National Eye Institute (R01EY021797, R01EY028557, and 5P30EY000331) and an unrestricted grant from Research to Prevent Blindness.

References

[1] Etodolac, LiverTox: Clinical and Research Information on Drug-Induced Liver Injury, 2012.
[2] N. Inoue, et al., The enantiomers of etodolac, a racemic anti-inflammatory agent, play different roles in efficacy and gastrointestinal safety, Biol. Pharm. Bull. 34 (2011) 655–659, https://doi.org/10.1248/bpb.34.655.
[3] D.R. Brocks, F. Jamali, The pharmacokinetics of etodolac enantiomers in the rat - lack of pharmacokinetic interaction between enantiomers, Drug Metab. Dispos. 18 (1990) 471–475.
[4] H.J. Lee, N.X. Wang, D.L. Shi, J.J. Zheng, Sulindac inhibits canonical Wnt signaling by blocking the PDZ domain of the protein dishevelled, Angew. Chem. Int. Ed. 48 (2009) 6448–6452, https://doi.org/10.1002/anie.200902981.
[5] R. Nusse, H. Clevers, Wnt/beta-Catenin signaling, disease, and emerging therapeutic modalities, Cell 169 (2017) 985–999, https://doi.org/10.1016/j.cell.2017.05.016.
[6] C. Zhang, et al., A small-molecule Wnt mimic improves human limbal stem cell ex vivo expansion, iScience 23 (2020), 101075, https://doi.org/10.1016/j.isci.2020.101075.
[7] S. Gonzalez, D. Oh, E.R. Baclagon, J.J. Zheng, S.X. Deng, Wnt signaling is required for the maintenance of human limbal stem/progenitor cells in vitro, Invest. Ophthalmol. Vis. Sci. 60 (2019) 107–112, https://doi.org/10.1167/iovs.18-25740.
[8] M.N. Nakatsu, et al., Wnt/beta-catenin signaling regulates proliferation of human cornea epithelial stem/progenitor cells, Invest. Ophthalmol. Vis. Sci. 52 (2011) 4734–4741, https://doi.org/10.1167/iovs.10-6486.
[9] H.J. Lee, et al., Structure-based discovery of novel small molecule Wnt signaling inhibitors by targeting the cysteine-rich domain of frizzled, J. Biol. Chem. 290 (2015) 30596–30606, https://doi.org/10.1074/jbc.M115.673202.
[10] T.A. Halgren, et al., Glide: a new approach for rapid, accurate docking and scoring. 2. Enrichment factors in database screening, J. Med. Chem. 47 (2004) 1750–1759, https://doi.org/10.1021/jm030644s.
[11] R.A. Friesner, et al., Glide: a new approach for rapid, accurate docking and scoring. 1. Method and assessment of docking accuracy, J. Med. Chem. 47 (2004) 1739–1749, https://doi.org/10.1021/jm0306430.
[12] Y. Wang, H. Chang, A. Rattner, J. Nathans, Frizzled receptors in development and disease, Curr. Top. Dev. Biol. 117 (2016) 113–139, https://doi.org/10.1016/bs.ctdb.2015.11.028.
[13] P. Kozielewicz, et al., Structural insight into small molecule action on Frizzleds, Nat. Commun. 11 (2020), https://doi.org/10.1038/s41467-019-14149-3.
[14] H. Chen, et al., Development of potent, selective surrogate WNT molecules and their application in defining frizzled requirements, Cell Chem. Biol. 27 (2020) 598–+, https://doi.org/10.1016/j.chembiol.2020.02.009.
[15] C.Y. Janda, et al., Surrogate Wnt agonists that phenocopy canonical Wnt and beta-catenin signalling, Nature 545 (2017) 234, https://doi.org/10.1038/nature22306.
[16] Y. Tao, et al., Tailored tetravalent antibodies potently and specifically activate Wnt/Frizzled pathways in cells, organoids and mice, Elife 8 (2019), https://doi.org/10.7554/eLife.46134.
[17] A. Koval, V.L. Katanaev, Platforms for high-throughput screening of Wnt/Frizzled antagonists, Drug Discov. Today 17 (2012) 1316–1322, https://doi.org/10.1016/j.drudis.2012.07.007.
[18] C.E. Dann, et al., Insights into Wnt binding and signalling from the structures of two Frizzled cysteine-rich domains, Nature 412 (2001) 86–90, https://doi.org/10.1038/35083601.
[19] N. Muller, et al., Stereoselective binding of etodolac to human serum-albumin, Chirality 4 (1992) 240–246, https://doi.org/10.1002/chir.530040407.
[20] Etodolac Tablet, Film Coated, STAT Rx USA LLC, National Library of Medicine, 2012.
[21] C.D. Silva, et al., Enantioselective analysis of etodolac in human plasma by LC-MS/MS: application to clinical pharmacokinetics, J. Pharmaceut. Biomed. 120 (2016) 120–126, https://doi.org/10.1016/j.jpba.2015.12.009.
[22] V. Ellerkamp, et al., Pharmacological inhibition of beta-catenin in hepatoblastoma cells, Pediatr. Surg. Int. 29 (2013) 141–149, https://doi.org/10.1007/s00383-012-3237-9.

[23] J. Behari, et al., R-Etodolac decreases beta-catenin levels along with survival and proliferation of hepatoma cells, J. Hepatol. 46 (2007) 849–857, https://doi.org/10.1016/j.jhep.2006.11.017.
[24] D. Lu, et al., Activation of the Wnt signaling pathway in chronic lymphocytic leukemia, Proc. Natl. Acad. Sci. U. S. A. 101 (2004) 3118–3123, https://doi.org/10.1073/pnas.0308648100.
[25] S.K. Kolluri, et al., The R-enantiomer of the nonsteroidal antiinflammatory drug etodolac binds retinoid X receptor and induces tumor-selective apoptosis, Proc. Natl. Acad. Sci. U. S. A. 102 (2005) 2525–2530, https://doi.org/10.1073/pnas.0409721102.
[26] D. Lu, H.B. Cottam, M. Corr, D.A. Carson, Repression of beta-catenin function in malignant cells by nonsteroidal antiinflammatory drugs, Proc. Natl. Acad. Sci. U. S. A. 102 (2005) 18567–18571, https://doi.org/10.1073/pnas.0509316102.
[27] T. Umemoto, et al., Limbal epithelial side-population cells have stem cell-like properties, including quiescent state, Stem Cell. 24 (2006) 86–94, https://doi.org/10.1634/stemcells.2005-0064.
[28] C. Bonnet, et al., Human limbal epithelial stem cell regulation, bioengineering and function, Prog. Retin. Eye Res. (2021), 100956, https://doi.org/10.1016/j.preteyeres.2021.100956.
[29] H. Yasui, et al., R-etodolac and a novel indole-pyran structural analog, SDX-308, induce cytotoxicity and overcome drug resistance in multiple myeloma, Blood 106 (2005), 453a-453a.
[30] S. Murata, et al., Etodolac improves 5-FU sensitivity of head and neck cancer cells through inhibition of thymidylate synthase, Anticancer Res. 31 (2011) 2893–2898.
[31] F.J. Huttner, et al., Pancreatic resection with perioperative drug repurposing of propranolol and etodolac: trial protocol of the phase-II randomised placebo controlled PROSPER trial, BMJ Open 10 (2020), https://doi.org/10.1136/bmjopen-2020-040406.
[32] R. Haider, et al., Perioperative COX2 and beta-adrenergic blockade improves biomarkers of tumor metastasis, immunity, and inflammation in colorectal cancer: a randomized controlled trial, Cancer-Am. Cancer Soc. 126 (2020) 3991–4001, https://doi.org/10.1002/cncr.32950.